



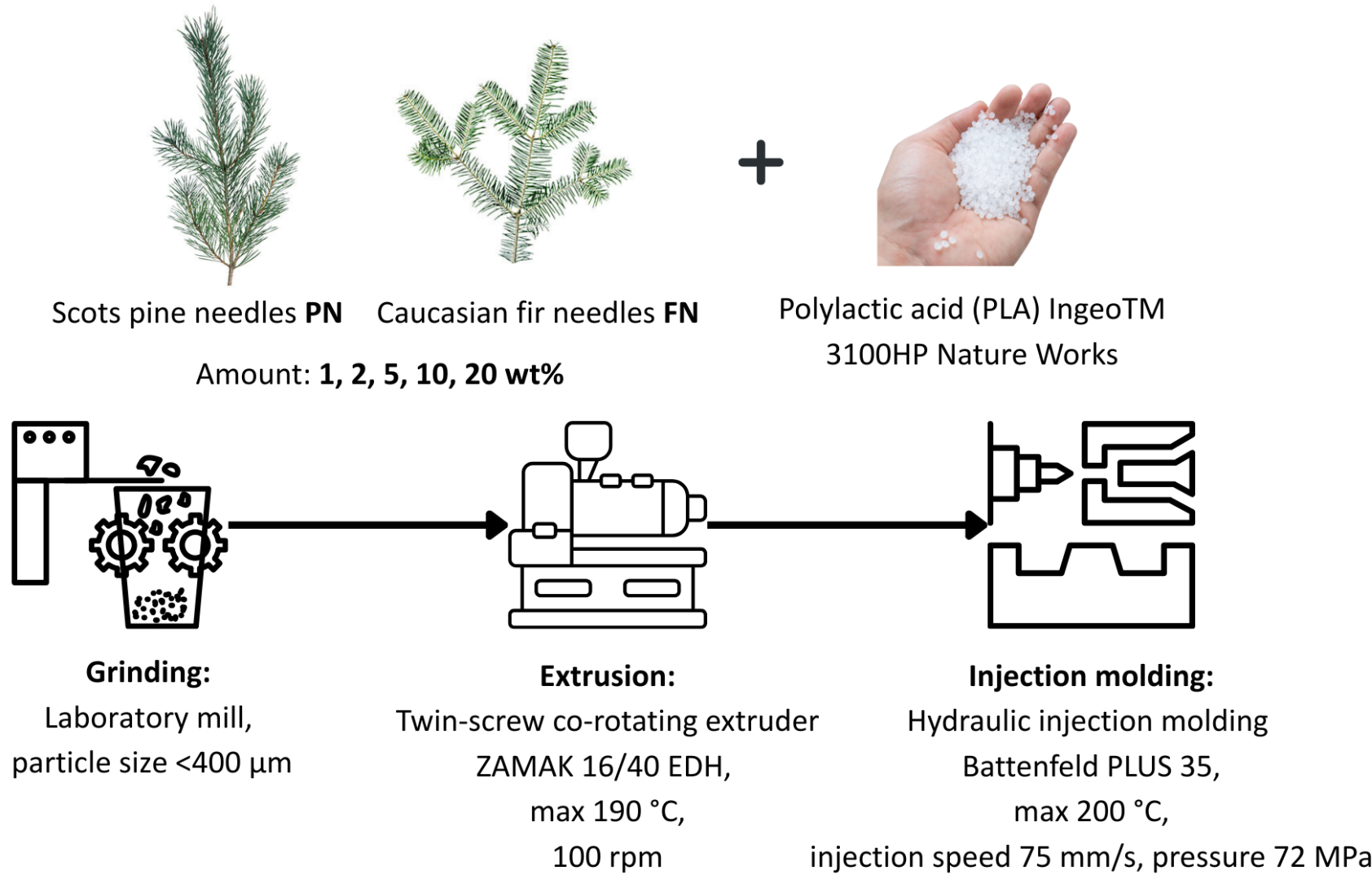
Discovering the potential of using coniferous tree needles Scots pine and Caucasian fir as functional fillers for PLA composites



Joanna Aniśko-Michalak¹, Mateusz Barczewski¹

¹ Poznan University of Technology, Faculty of Mechanical Engineering Institute of Materials Technology, Piotrowo 3, 61-138 Poznan, Poland, ORCID: MB: 0000-0003-1451-6430; JA-M: 0000-0002-4638-8819

MATERIALS AND PROCESSING



METHODS

Chemical composition tests identified cellulose, lignin, hemicelluloses, and extractives in organic solvents. Antioxidant properties were evaluated using DPPH and Folin-Ciocalteu assays. Thermogravimetric analysis (TGA), Differential Scanning Calorimetry (DSC), and Scanning Electron Microscopy (SEM) examined thermal and structural characteristics of PLA and its composites. Crystallization behavior was analyzed via polarized light optical microscopy (POM). Tensile testing, conducted per ISO 527, assessed mechanical properties. Surface wettability and water uptake were also measured.

Table 1. Chemical composition and results of antioxidant activity evaluation of fillers.

Parameter	Unit	PN	FN
Chemical composition			
Cellulose	[%]	38.17	26.14
Hemicellulose	[%]	12.89	15.76
Lignin	[%]	24.46	35.87
Mineral substances	[%]	2.35	4.95
Extractives	[%]	35.10	31.32
Total phenolic content			
Gallic acid equivalent	[mg/g dry mass]	35.07 ± 0.34	59.45 ± 3.83
Antioxidant activity			
Inhibition	[%]	33.52 ± 0.49	87.26 ± 1.08
Trolox equivalent	[mg/g dry mass]	49.00 ± 0.89	146.19 ± 1.95

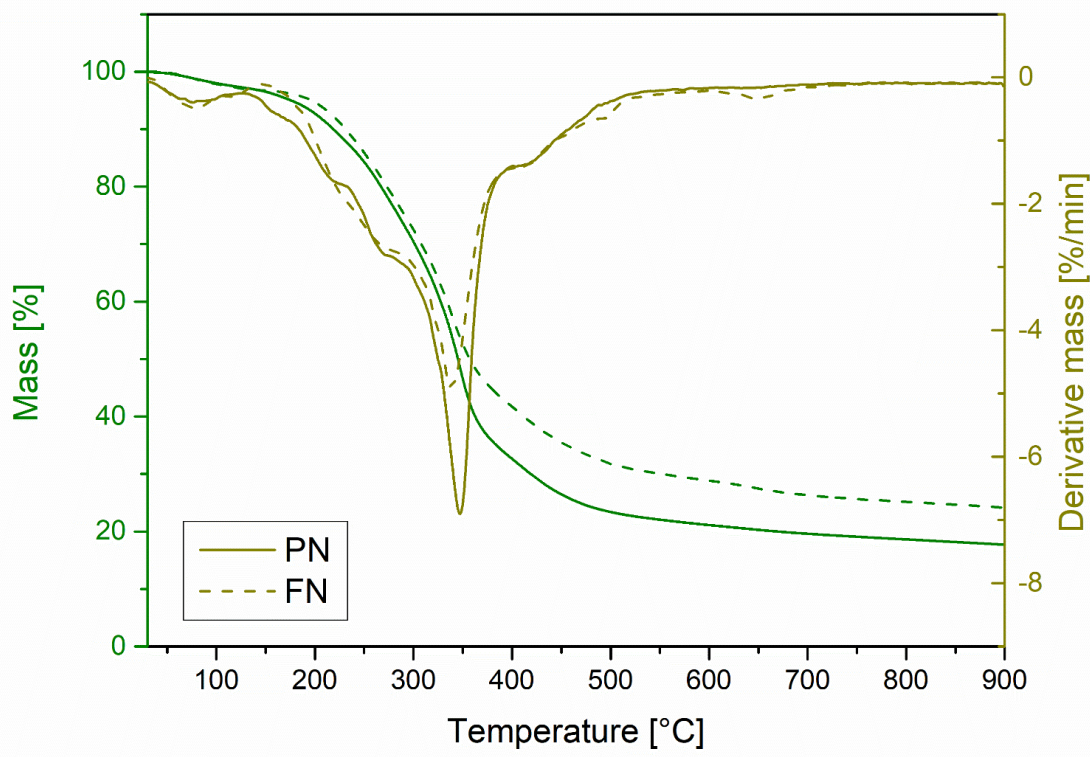


Fig. 1. Thermogravimetric and DTG curves at nitrogen atmosphere for biomass fillers.

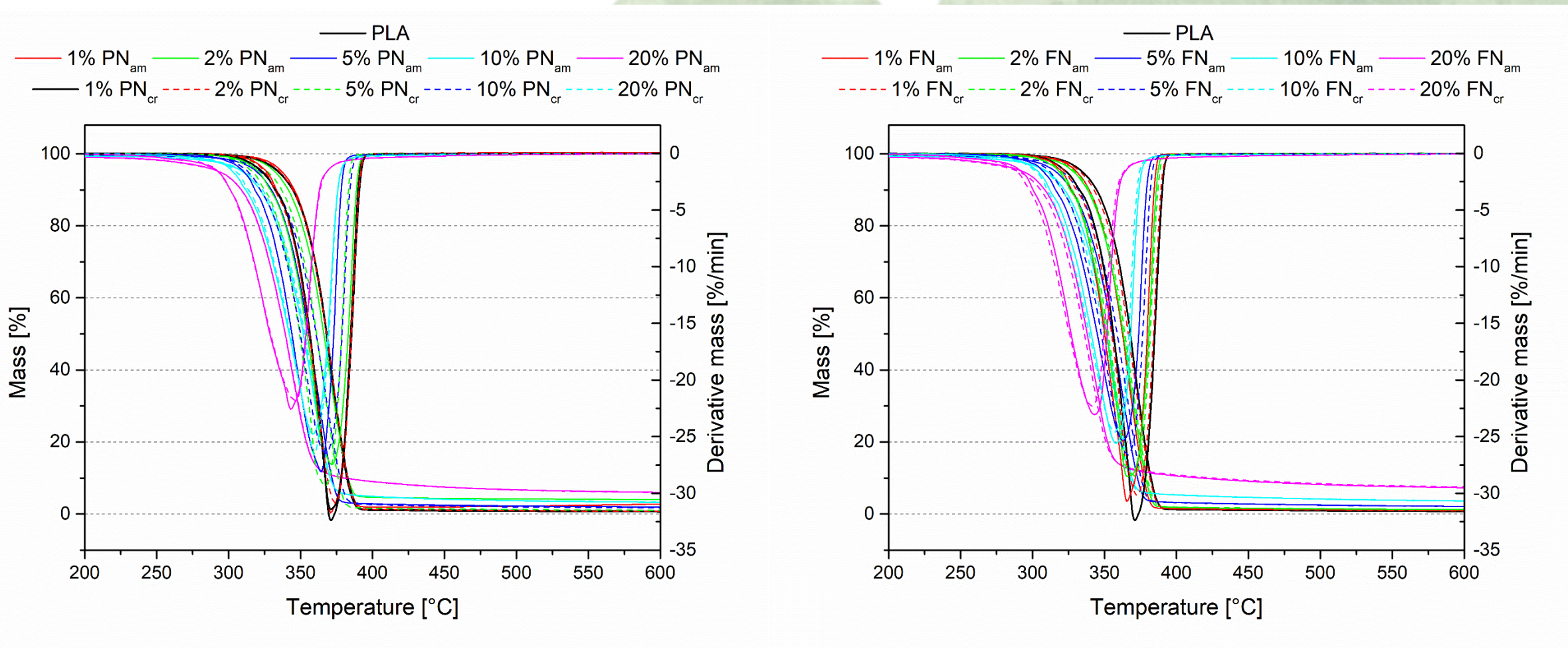


Fig. 2. Thermogravimetric curves of composites samples before and after annealing.

Table 2. Oxygen onset temperature (OOT) values determined for amorphous and crystallized PLA-based composites.

Oxygen onset temperature [°C]				
Filler content [%]	Amorphous (am)		Crystallized (cr)	
	PN	FN	PN	FN
0	223.3		222.6	
1	251.6	246.3	257.9	244.7
2	270.5	271.4	269.2	269.8
5	286.2	282.9	290.3	282.3
10	264.9	258.5	251.0	251.4
20	252.9	246.2	232.6	232.7

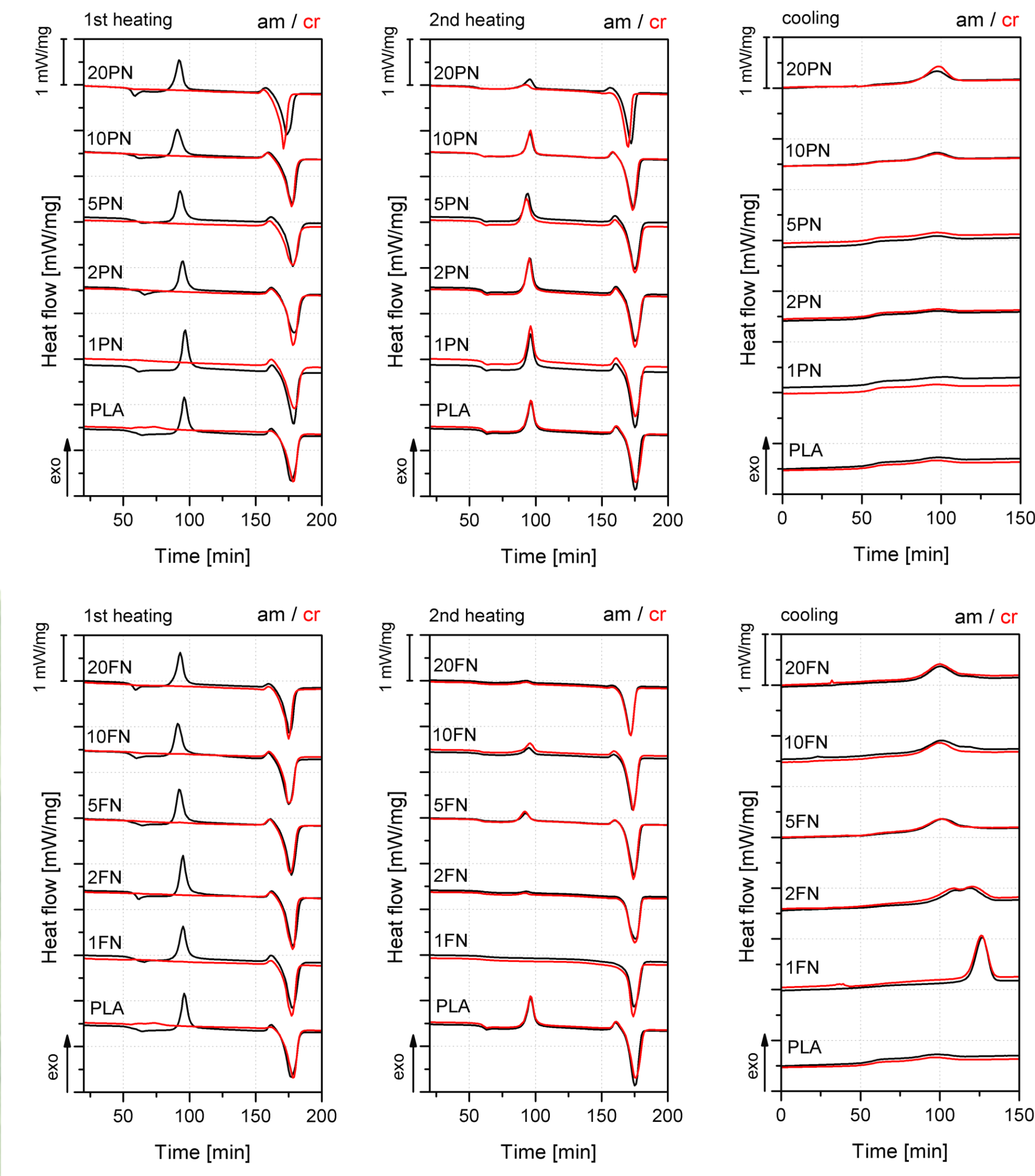


Fig. 5. DSC thermograms of PLA and PN-/FN-composites.

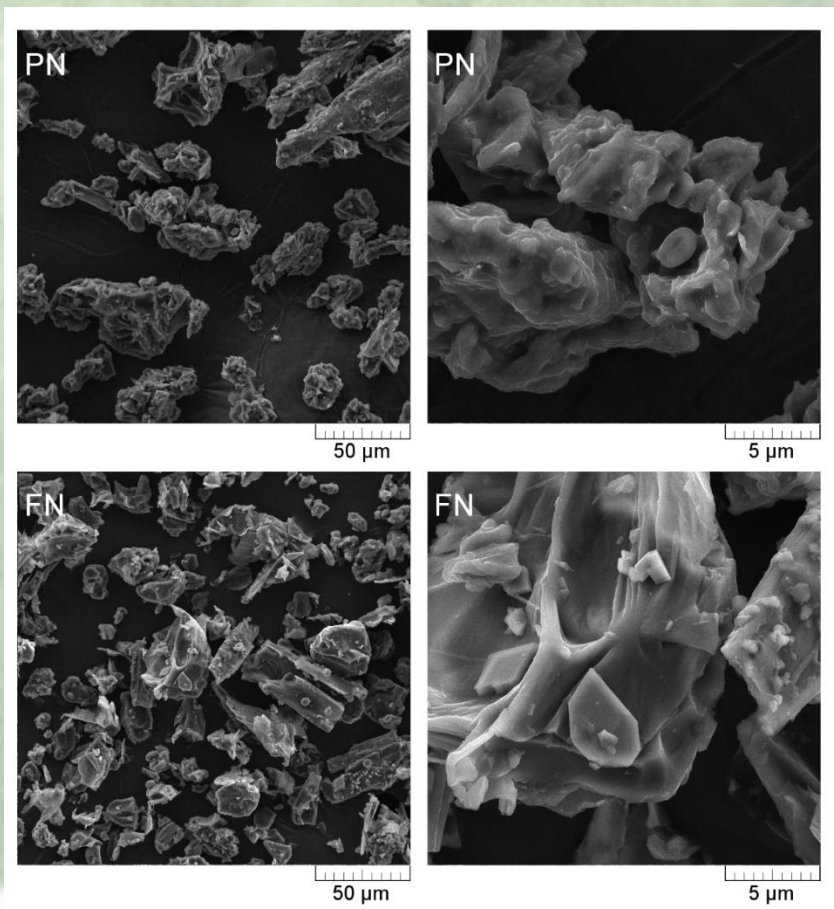


Fig. 3. SEM images of ground and sieved fillers.

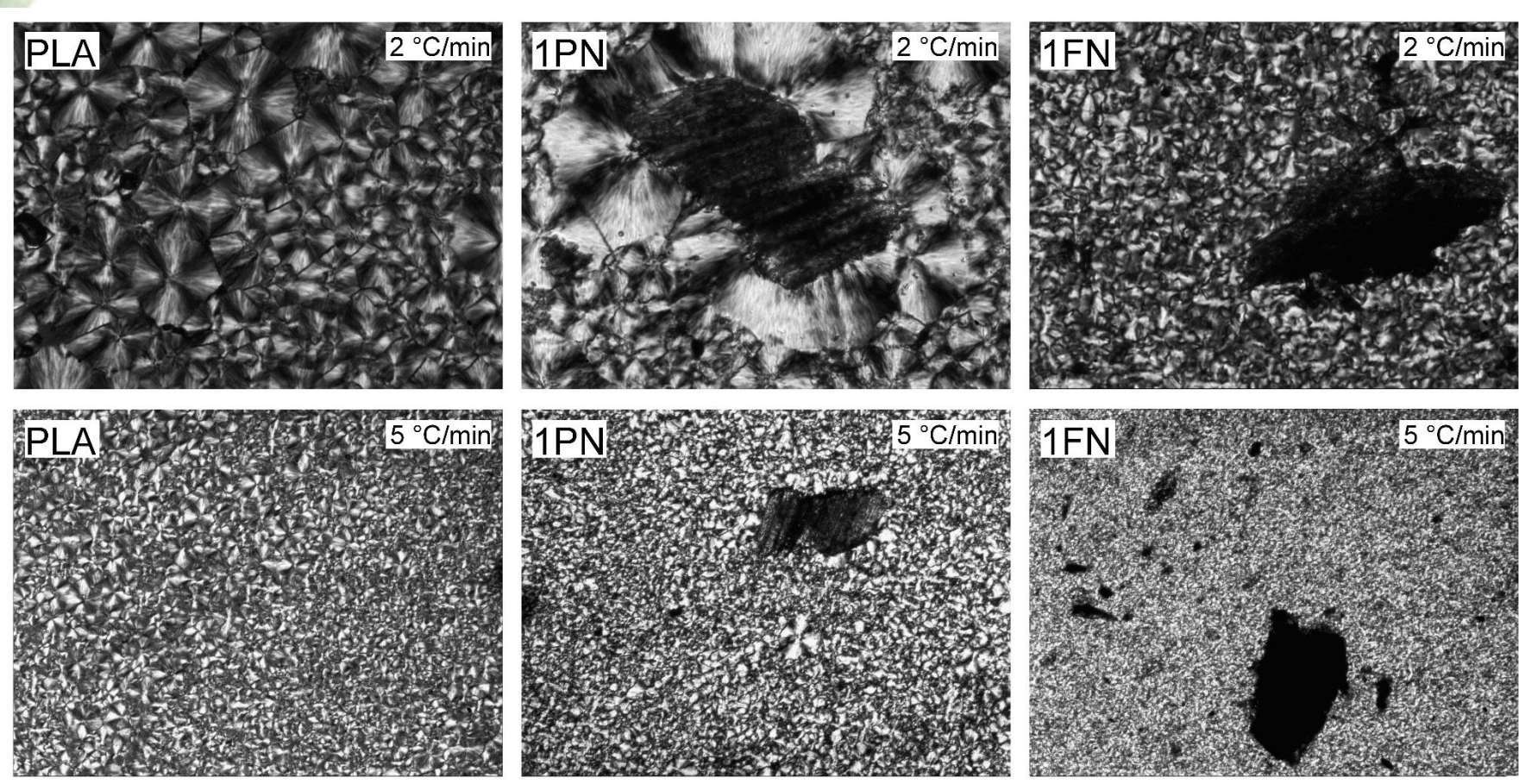


Fig. 4. POM images after crystallizing selected samples at the heating stage with 2 and 5 °C/min cooling rates.

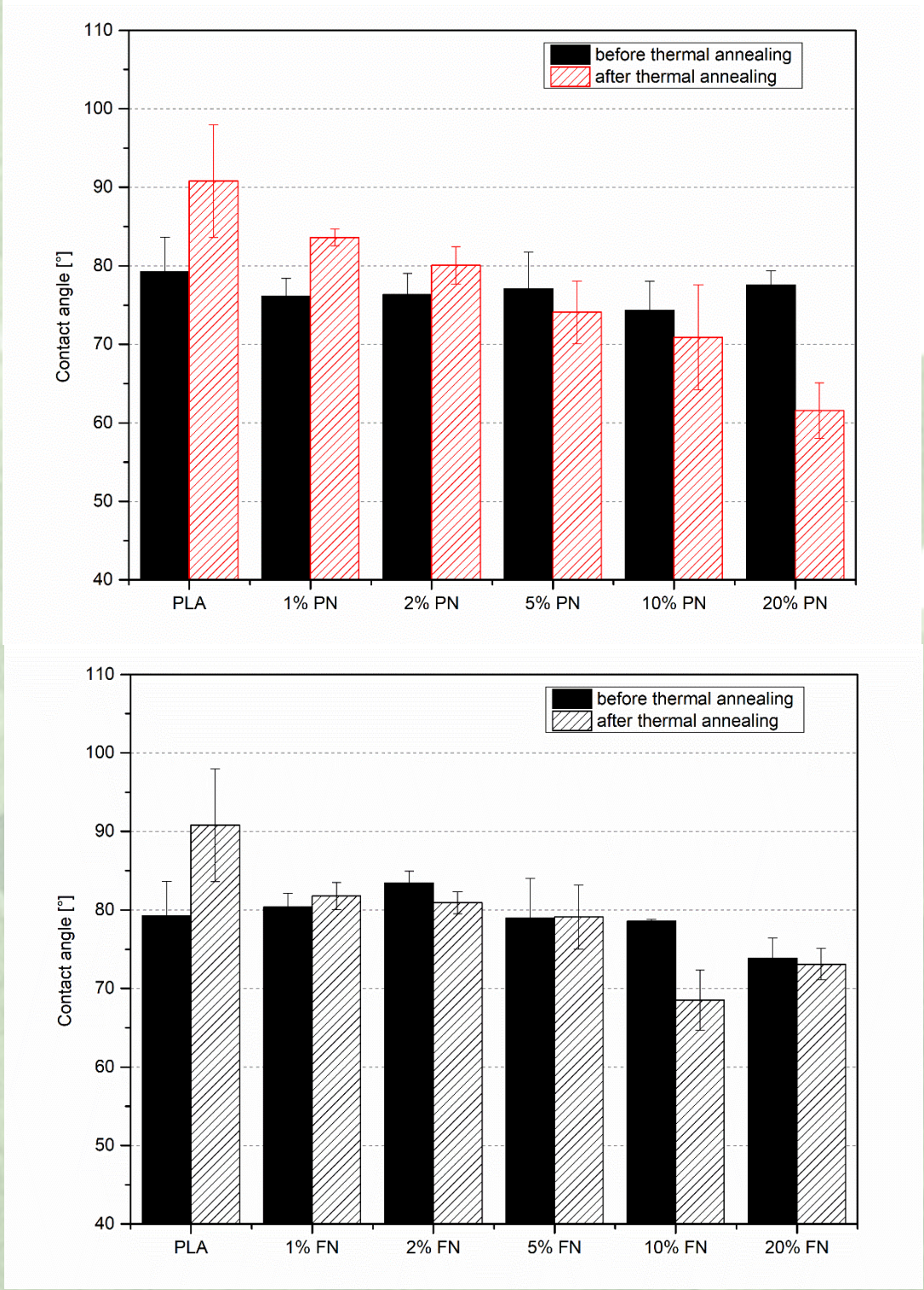


Fig. 6. Water contact angle for PLA and PLA-PN/FN before and after annealing.

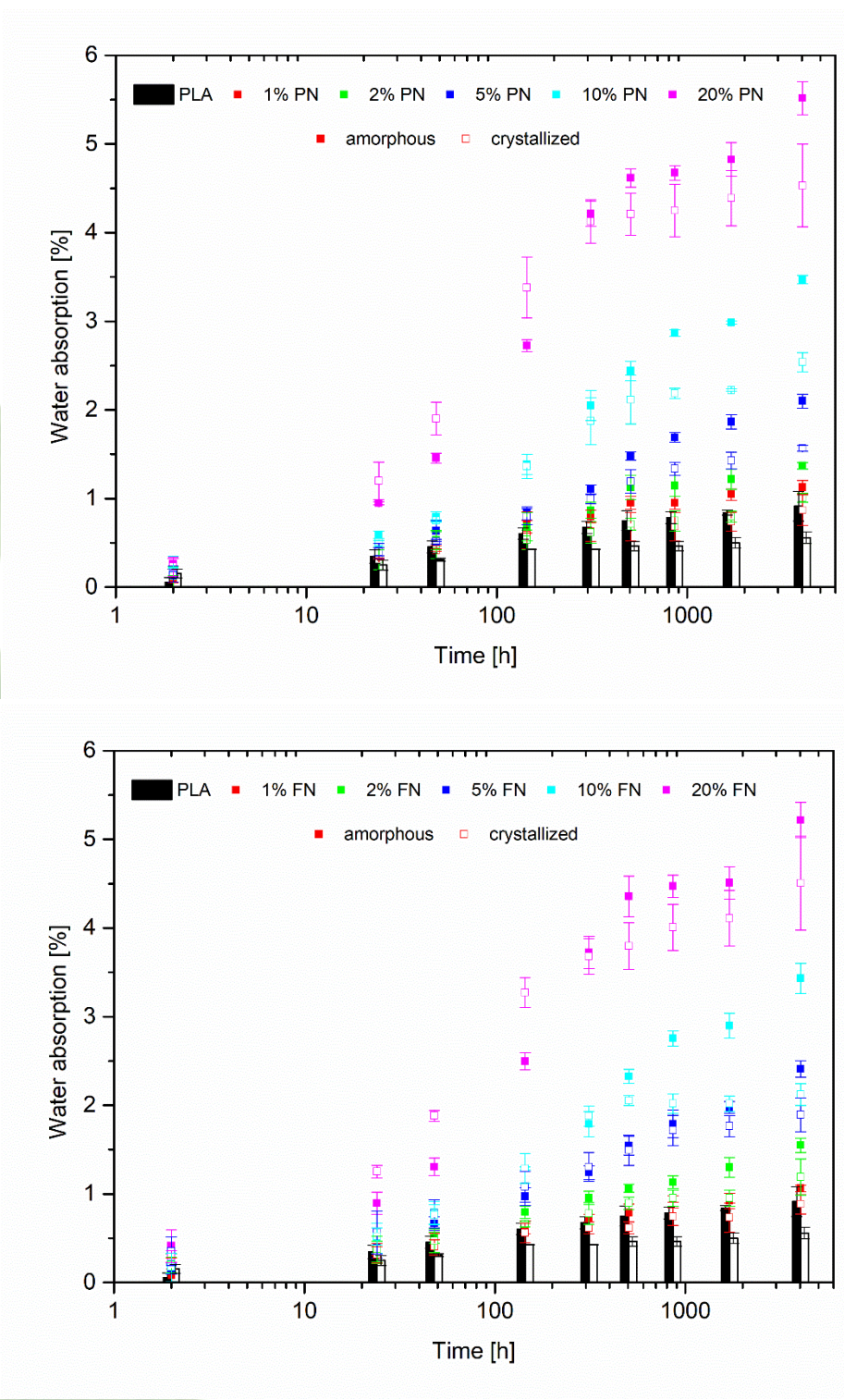


Fig. 7. Static water absorption results for PLA composites with pine and fir needles.

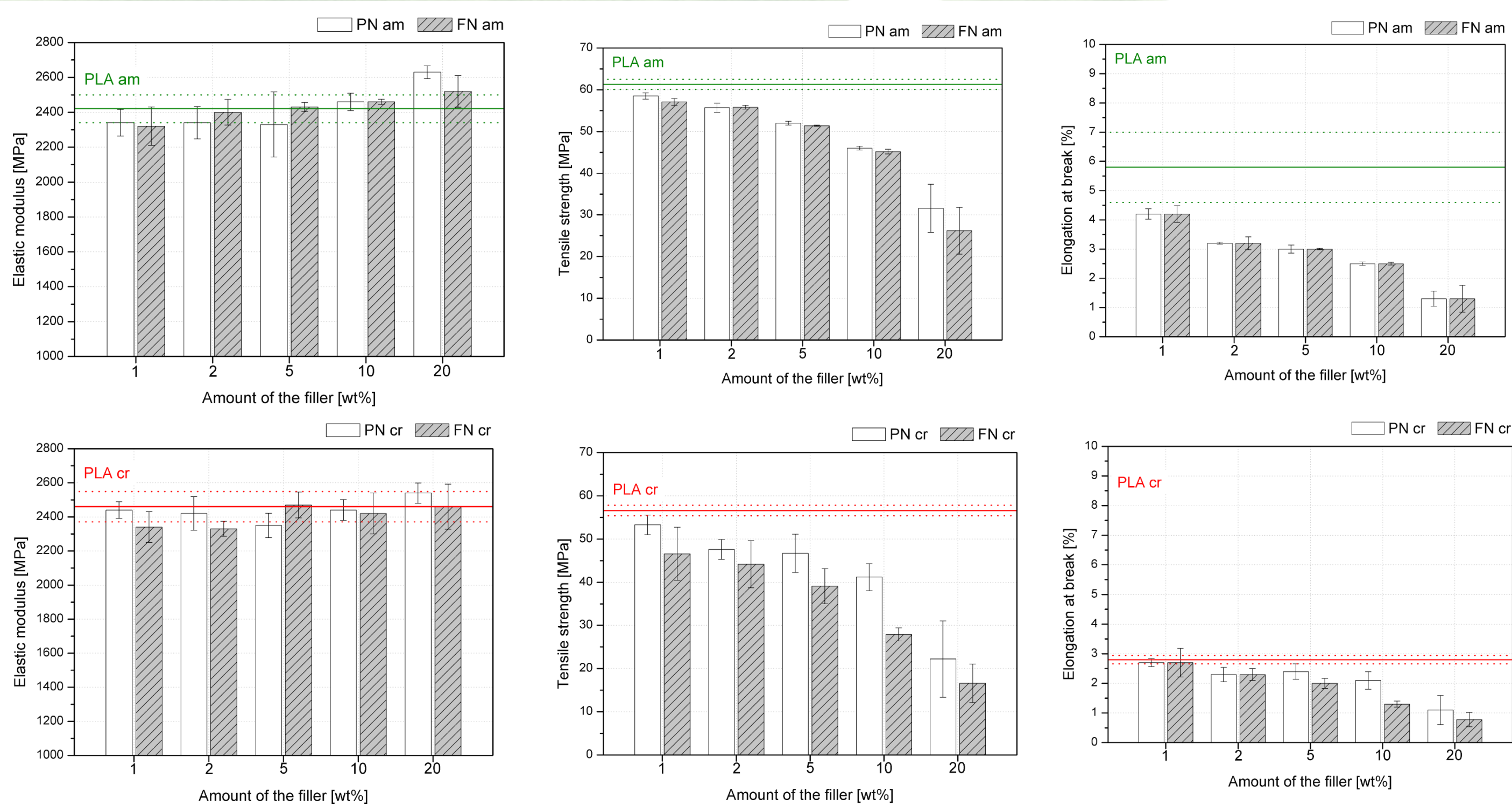


Fig. 8. Mechanical properties of PLA and PN-/FN-filled composites determined by static tensile test.

